Mechanistic Studies of the Oxygen-Mediated Oxidation of Nitrosylhemoglobin†

Susanna Herold* and Gabriele Röck

Laboratorium für Anorganische Chemie, Eidgenössische Technische Hochschule, ETH Hönggerberg, CH-8093 Zürich, Switzerland

Received November 15, 2004; Revised Manuscript Received March 4, 2005

ABSTRACT: Nitrosylhemoglobin ($HbFe^{II}NO$) has been shown to be generated in vivo from the reaction of deoxyHb with $NO^{\bullet}$ as well as with nitrite. Despite the physiological importance attributed to this form of Hb, its reactivity has not been investigated in detail. In this study, we showed that the rate of oxidation of $HbFe^{II}NO$ by O_2 does not depend on the O_2 concentration. The reaction time courses had to be fitted to a two-exponential expression, and the obtained rates were approximately 2×10^{-4} and 1×10^{-4} s^{-1}, respectively. In the presence of the allosteric effector inositol hexaphosphate (IHP), the value for the fast component of the rate was significantly larger (44×10^{-4} s^{-1}) whereas that for the slow step was only slightly higher (2.5×10^{-4} s^{-1}). Moreover, we found that both in the absence and in the presence of IHP the rate of the O_2-mediated oxidation of $HbFe^{II}NO$ is essentially identical to that of $NO^{\bullet}$ dissociation from $HbFe^{II}NO$, determined under analogous conditions by replacement of $NO^{\bullet}$ with CO in the presence of an excess of dithionite. Taken together, our data show that the reaction between O_2 and $HbFe^{II}NO$ proceeds in three steps via dissociation of $NO^{\bullet}$ (rate-determining step), binding of O_2 to deoxyHb, and $NO^{\bullet}$-mediated oxidation of oxyHb to metHb and nitrate.

Nitrogen monoxide produced by the endothelial isoform of nitric oxide synthase (eNOS)[1] is responsible for the regulation of blood vessel tone and inhibits platelet aggregation as well as lipid peroxidation (*1*). A large fraction of this $NO^{\bullet}$ reacts with blood components, in particular with hemoglobin (Hb) encapsulated within the red blood cells (RBCs). Because of the high concentration of oxyHb in the RBCs and the large value of the second-order rate constant for the irreversible reaction between oxyHb and $NO^{\bullet}$ [$(8.9 \pm 0.3) \times 10^7$ M^{-1} s^{-1} (per heme), at pH 7.0 and 20 °C (*2*)], oxyHb was initially considered as the main sink for $NO^{\bullet}$ in the vascular system (*3*−*5*). This hypothesis was first challenged by Stamler and co-workers, who proposed that $NO^{\bullet}$ is transported in the vasculature by Hb as a *S*-nitroso adduct of a highly conserved cysteine residue in the β-chain (Cysβ93) (*6*, *7*). This so-called SNO-Hb was suggested to be formed by intramolecular transfer from nitrosylHb ($HbFe^{II}NO$), the product from the reaction of $NO^{\bullet}$ with deoxyHb within the RBCs (*6*, *7*). Recent studies have revealed the existence of a further pathway for SNO-Hb and $HbFe^{II}NO$ formation in vivo. It has been reported that deoxyHb can act as a nitrite reductase and, thus, generate $NO^{\bullet}$ and possibly $HbFe^{II}NO$ as well as SNO-Hb (*8*, *9*). In both systems, a potential pathway for recycling the $NO^{\bullet}$ transported by Hb may be represented by $NO^{\bullet}$ dissociation from $HbFe^{II}NO$.

The corresponding myoglobin (Mb) complex $MbFe^{II}NO$ is the primary pigment in cured meat products, in which it is generated by reaction of oxyMb with nitrite in the presence of reducing agents (*10*). $MbFe^{II}NO$ has been shown to inhibit lipid peroxidation through radical scavenging (*11*) and to prevent the formation of the high valent oxoiron(IV) form of Mb ($MbFe^{IV}{=}O$), since reaction of H_2O_2 with $MbFe^{II}NO$ produces directly metMb. The reaction between $MbFe^{II}NO$ and O_2 has been proposed to proceed in two steps via the formation of a N-bound peroxynitrite−metmyoglobin complex [$MbFe^{III}N(O)OO^-$] (*12*), which displays a UV/vis absorbance spectrum very similar to that of the corresponding O-bound metmyoglobin complex ($MbFe^{III}OONO$) (*2*). In contrast, recent reinvestigation of the mechanism of this reaction suggested that the bound $NO^{\bullet}$ is displaced by O_2 in a reversible ligand-exchange reaction prior to an irreversible electron transfer (*13*). Thermodynamic data indicated that the ligand exchange is a dissociative process somewhat assisted by an entering O_2 molecule (*13*). The released $NO^{\bullet}$ is proposed to be trapped in a protein cavity and thus to be unavailable for reaction with noncoordinated O_2 in the bulk solution (*13*).

Despite the physiological importance attributed to $HbFe^{II}NO$, the mechanism of its reaction with O_2 has not been studied in detail. We have previously reported that this reaction leads to the formation of small amounts of SNO-Hb (*14*). In the present work, we studied the influence of the O_2 and CO_2 concentrations on the rate of the O_2-mediated oxidation of $HbFe^{II}NO$. The lack of influence of the O_2 concentration on the reaction rate suggested that the rate-determining step of this reaction is dissociation of $NO^{\bullet}$ from $HbFe^{II}NO$. Investigations in the presence of the allosteric

† This work was supported by the Swiss National Science Foundation.

* To whom correspondence should be addressed. E-mail: herold@inorg.chem.ethz.ch. Tel: (41) (1) 632 28 58. Fax: (41) (1) 632 10 90.

[1] Abbreviations: Hb, hemoglobin; $HbFe^{II}$, deoxyhemoglobin (deoxyHb); $HbFeO_2$, oxyhemoglobin (oxyHb); metHb, iron(III) hemoglobin; $HbFe^{IV}{=}O$, oxoiron(IV) hemoglobin (ferrylHb); $HbFe^{II}NO$, nitrosylhemoglobin; IHP, inositol hexaphosphate; Mb, myoglobin; $MbFeO_2$, oxymyoglobin (oxyMb); metMb, iron(III) myoglobin; $MbFe^{IV}{=}O$, oxoiron(IV) myoglobin (ferrylMb); $MbFe^{II}NO$, nitrosylmyoglobin; eNOS, endothelial nitric oxide synthase; RBC, red blood cell; SNO-Hb, hemoglobin with Cysβ93 S-nitrosated.

10.1021/bi0475929 CCC: $30.25
Published on Web 03/31/2005

effector inositol hexaphosphate (IHP) confirmed that the observed rate constant for the oxidation of $HbFe^{II}NO$ by O_2 was identical to that of $NO^{\bullet}$ dissociation from $HbFe^{II}NO$, measured under analogous conditions by $NO^{\bullet}$ replacement with CO in the presence of an excess dithionite.

EXPERIMENTAL PROCEDURES

Reagents. Buffer solutions (0.1 M) were prepared from K_2HPO_4/KH_2PO_4 (Fluka) with deionized Milli-Q water and always contained 0.1 mM diethylenetriaminepentaacetic acid (DTPA, Sigma). Sodium dithionite, sulfanilamide, and ammonium sulfamate were obtained from Fluka. Sodium bicarbonate was purchased from Merck. The dipotassium salt of inositol hexaphosphoric acid (IHP) was obtained from Sigma. Nitrogen monoxide was obtained from Linde and passed through a NaOH solution as well as a column of NaOH pellets to remove higher nitrogen oxides before use. Aqueous $NO^{\bullet}$-saturated solutions (2 mM) were prepared as described previously (*14*) and, when needed, diluted with degassed buffer in gastight SampleLock Hamilton syringes. Carbon monoxide was purchased from PanGas.

Protein Solutions. A purified human oxyhemoglobin (oxyHb) stock solution (57 mg/mL solution of HbA_0 with approximately 1.1% metHb) was a kind gift from APEX Bioscience, Inc. DeoxyHb solutions were prepared by thoroughly degassing ice-cooled oxyHb solutions with a constant flow of argon over the surface of the solution while gently stirring. Approximately half an hour before carrying out the experiments, the deoxyHb solution was allowed to warm to room temperature (under argon). The quantitative formation of deoxyHb was confirmed by recording a UV/vis spectrum [$\lambda_{max} = 555$ nm, $\epsilon_{555} = 12.5\ mM^{-1}\ cm^{-1}$ (*15*)]. $HbFe^{II}NO$ solutions were prepared by adding 1 equiv of $NO^{\bullet}$ (from a saturated aqueous solution) to a deoxyHb solution. The final concentration of the $HbFe^{II}NO$ solution was determined by measuring its absorbance at 418, 544, and 572 nm ($\epsilon_{418} = 130\ mM^{-1}\ cm^{-1}$, $\epsilon_{544} = 11.4\ mM^{-1}\ cm^{-1}$, and $\epsilon_{572} = 11.4\ mM^{-1}\ cm^{-1}$) (*15*). The concentrations of the Hb solutions are always expressed per heme.

Analysis of the S-Nitrosothiol Content with the Saville Assay. The *S*-nitrosothiol content was determined with the Saville assay as described in detail elsewhere (*14*, *16*). In brief, we used the following set of reagents: solution A (1 mM ammonium sulfamate in 0.5 M HCl), solution B (1% sulfanilamide in 0.5 M HCl), solution C (1% sulfanilamide and 0.2% $HgCl_2$ in 0.5 M HCl), and solution D [0.02% *N*-(1-naphthyl)ethylenediamine dihydrochloride in 0.5 M HCl]. All of the absorption spectra required for the quantification of *S*-nitrosothiols were collected in 1 cm cells with a UVIKON 820 spectrophotometer.

SNO-Hb Formation from the Reaction of DeoxyHb with $NO^{\bullet}$. All reactions were carried out at room temperature in phosphate buffer (0.1 M), pH 7.0−7.2, which contained 0.1 mM DTPA, in sealable cells for anaerobic applications. DeoxyHb (ca. 50 μM) was first prepared as described above. Depending on the equivalents of $NO^{\bullet}$ required (1 or 0.1 equiv relative to the heme concentration; that is, 2 or 0.2 equiv relative to the Cysβ93 concentration), 5 or 50 μL of a $NO^{\bullet}$-saturated solution (2 mM) was rapidly added to the deoxyHb solution while vortex mixing. The reaction mixture was allowed to react for either 10 or 60 min. Finally, the cell was opened, and the solution was transferred into another vial and was analyzed immediately or after 10 min for SNO-Hb with the Saville assay (under aerobic conditions).

To confirm the requirement of O_2 for *S*-nitrosothiol formation from $HbFe^{II}NO$, as a control we quantified the SNO-Hb produced from the reaction of deoxyHb with $NO^{\bullet}$ by carrying out the Saville analysis under strictly anaerobic conditions, by thoroughly degassing each of the solutions containing the reagents.

To find out whether carbon dioxide present in air influences the SNO-Hb yields, in an additional set of experiments we added 1 mL of a 440 μM O_2 solution to 1 mL of a 100 μM $HbFe^{II}NO$ solution in a sealed cell for anaerobic applications (instead of exposing the $HbFe^{II}NO$ solution to air). The final O_2 concentration (220 μM) corresponded approximately to that of an air-saturated aqueous solution. The reaction mixture was then treated either immediately or after 10 min with degassed ammonium sulfamate (under anaerobic conditions). Finally, the last steps of the Saville analysis to determine the Cysβ93−NO content were carried out under aerobic conditions.

Spectroscopic Studies of the Reaction of $HbFe^{II}NO$ with Dioxygen. The reactions of $HbFe^{II}NO$ with O_2 were all carried out at room temperature in sealable cells for anaerobic applications and followed spectrophotometrically (in the range 450−650 nm) with an Analytic Jena Specord 100 or an Analytic Jena Specord 200 instrument for 14−24 h. Spectra were mostly collected every 4 min. In all experiments the final protein concentration was 45−50 μM. One equivalent of $NO^{\bullet}$ was added to a deoxyHb solution, and a UV/vis spectrum was recorded to confirm the quantitative formation of $HbFe^{II}NO$. Then, 2−2.7 mL of an oxygen-containing solution (200−1300 μM in 0.1 M phosphate buffer) was added with a gastight SampleLock Hamilton syringe. The final volume was always at least 4 mL, to keep the headspace in the cell at a minimum. For instance, for the experiments with a final oxygen concentration of ~850 μM we added 2.7 mL of a saturated O_2 solution (1.3 mM) to 1.3 mL of a $HbFe^{II}NO$ solution (about 160 μM). When a final oxygen concentration of ~100 μM was needed, the saturated O_2 solution was first diluted 1:6.5 in a gastight syringe with degassed buffer. Two milliliters of this diluted O_2 solution was added to 2 mL of a $HbFe^{II}NO$ solution (about 100 μM).

In some cases, instead of adding an O_2-containing solution, the $HbFe^{II}NO$ solution was allowed to react with air by just opening the cell. Alternatively, to accelerate diffusion of air into the reaction mixture, we transferred (under aerobic conditions) the $HbFe^{II}NO$ solution into a new (air-filled) cell and then started the measurement.

To investigate the influence of CO_2/bicarbonate on the oxidation rate of $HbFe^{II}NO$, we carried out a further set of reactions in the presence of an excess of added CO_2. For this purpose, we first treated the $HbFe^{II}NO$ solution with 10 or 100 μL of a 55 or 550 mM degassed sodium bicarbonate solution (in H_2O). Immediately after, we added the required amount of an O_2-containing solution and started the measurement. The final CO_2/bicarbonate concentrations were approximately in the range between 12 μM and 1.2 mM, calculated by using the value of 1.41×10^6 M for the hydration−dehydration equilibrium of CO_2 (*17*). In a last experiment, we determined the rate of oxidation of $HbFe^{II}NO$ by treating 1 mL of a 150 μM $HbFe^{II}NO$ solution

with 2 mL of air-saturated H_2O in a sealed cell (final O_2 concentration ~150 μM).

For the reactions in the presence of IHP, 20 μL of a degassed 50 mM IHP solution in H_2O was added to the $HbFe^{II}NO$ solution to give a final IHP concentration of 250 μM (5 equiv relative to the heme concentration). After 10 min, the O_2 solutions were added as described above. To measure more accurately the absorbance changes which occurred during the first 12 min of the reaction, for the experiments in the presence of IHP we also collected spectra every 7 s in a significantly narrower wavelength range (542−547 nm). These data were combined with the measurements over a longer time scale to obtain an accurate reaction time course at 544 nm.

Determination of the NO• Dissociation Rate from $HbFe^{II}NO$ by Replacement with CO. Replacement of the coordinated NO• in $HbFe^{II}NO$ by CO was followed spectrophotometrically in the range 450−650 nm with an Analytic Jena Specord 100 or an Analytic Jena Specord 200 instrument for 24 h. In most cases, spectra were collected at room temperature every 4 min. However, for the reactions in the presence of IHP, the first 12 min of the reaction was also studied by measuring a narrower wavelength range (470−490 nm) every 7 s. These data were then combined to get an accurate reaction time course at 480 nm.

$HbFe^{II}NO$ (500 μL of an ~440 μM solution in 0.1 M phosphte buffer, pH 7.2) was prepared in a sealable cell for anaerobic applications as described above. A 10 mM sodium dithionite solution (in 0.1 M phosphate buffer, pH 7.2) was prepared anaerobically and saturated with CO gas for 2 h. The replacement reaction was started by adding 3.8 mL of the CO-saturated dithionite solution to 500 μL of the $HbFe^{II}NO$ solution. The final CO and dithionite concentrations were 850 μm and 8.5 mM, respectively. For the reactions in the presence of IHP, 20 μL of a degassed 50 mM IHP solution in H_2O was added to the $HbFe^{II}NO$ solution to give a final IHP concentration of 250 μM. After 10 min, the CO solution was added as described above, and the measurement was started immediately.

Statistics. The experiments reported in this paper were carried out at least in triplicate on independent days. The results are given as mean values of at least three experiments plus or minus the corresponding standard deviation.

RESULTS

Kinetic Studies of the O_2-Mediated Oxidation of $HbFe^{II}NO$ in the Absence and Presence of CO_2 or IHP. The O_2-mediated oxidation of $HbFe^{II}NO$ was studied by UV/vis spectroscopy by following the absorbance changes that accompanied the reaction of $HbFe^{II}NO$ (45−50 μM) with different concentrations of O_2 (100−850 μM, in 0.1 M phosphate buffer, pH 7.2). The spectra were mostly collected every 4 min in the range 450−650 nm. As shown in Figure 1, upon addition of oxygen the spectrum of $HbFe^{II}NO$ (bold line) slowly converted to that of metHb (λ_{max} = 500 and 631 nm). The representative measurement depicted in Figure 1 shows that apparently the reaction proceeds without clean isosbestic points. However, careful analysis of the single spectra indicated the presence of two isosbestic points around 523 and 602 nm during the first 2−3 h of reaction. Since the measurements were carried out over several hours (up to 15−16 h), it is possible that the absence of isosbestic points throughout the whole reaction is simply due to the instability of the lamp and/or of the protein solution. Indeed, the deviations from the isosbestic points were normally in the range of 0−5 nm and were not always identical. For all oxygen concentrations studied, the last spectrum was essentially identical to that of metHb.

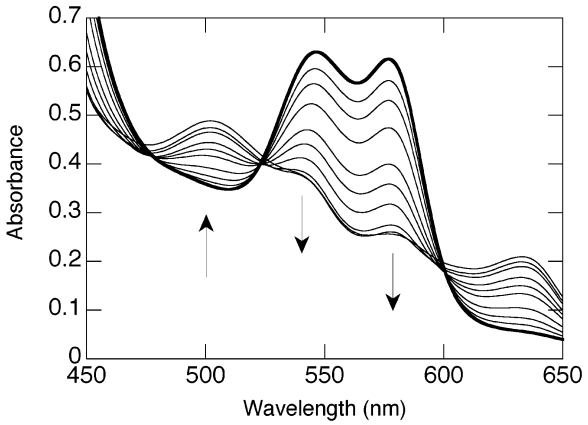

FIGURE 1: UV/vis spectra of the reaction of ~51 μM $HbFe^{II}NO$ with 650 μM O_2 in 0.1 M phosphate buffer, pH 7.2. Conversion of $HbFe^{II}NO$ (bold line) to metHb (λ_{max} = 500 and 631 nm). The spectra depicted were collected immediately, 16 min, 32 min, 1 h, 2 h, 3 h, 6 h, 9 h, 12.2 h, and 15.4 h after mixing.

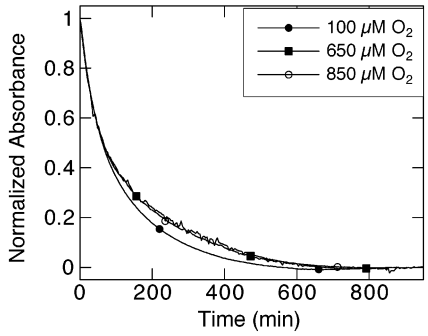

FIGURE 2: Normalized averaged time courses (at 544 nm) of the reactions of ~45 μM $HbFe^{II}NO$ with different amounts of O_2 (given in the legend) in 0.1 M phosphate buffer, pH 7.2. Spectra were collected every 4 min.

To determine the reaction rate, we usually extracted the reaction time courses at 544 nm, one of the wavelengths at which the absorbance changes between $HbFe^{II}NO$ and metHb were among the largest. Nearly identical rates were obtained by fitting the traces at 575 and 630 nm, two wavelengths close to the maxima of the spectra of $HbFe^{II}NO$ and metHb, respectively. It has been reported that there are differences between the spectrum of fully saturated $HbFe^{II}NO$ and that of partially nitrosylated hemoglobin (*18*). To avoid interferences of these further spectral changes, we also investigated the reaction time courses extracted at 450 and 590 nm, two wavelengths where these differences are minimal. Also, at these two wavelengths the results of the fits were identical to those measured at 544 nm. In all cases, the kinetic traces could be fitted reasonably well to a two-exponential expression. Deviation from the exponential decay, observed in some cases after several hours of reaction, was probably due to the instability of the lamp and/or denaturation of the protein. As shown in Figure 2, the apparent reaction rate did not depend significantly on the amount of O_2 added. The values of the two apparent reaction rates obtained from the fit of

Table 1: Observed Rate Constants for Reaction of $HbFe^{II}NO$ (50 μM) with Different Amounts of O_2 in the Absence or Presence of Different Amounts of CO_2 or 250 μM IHP and Comparison of the Values Obtained from the Fit with a Two-Exponential Expression with Those Calculated from the Linear Fit of the Logarithmic Plot (Given in Parentheses in Italic Type)

		rate constants ($\times 10^{-4}$ s^{-1})				
$[O_2]$ (μM)		$[CO_2]$ (μM)				[IHP] (μM)
		0	12	120	1200	250
100	fast	5 ± 1 (*2.0*)	4 ± 1 (*2.0*)	4 ± 1 (*1.9*)	7 ± 1 (*2.4*)	42 ± 1 (*43*)
	slow	1.1 ± 0.2 (*1.2*)	0.8 ± 0.2 (*1.1*)	0.9 ± 0.2 (*1.2*)	1.1 ± 0.1 (*1.1*)	2.5 ± 0.1 (*2.9*)
650	fast	5 ± 1 (*2.0*)	nd[a] nd	nd nd	nd nd	59 ± 1 (*45*)
	slow	0.8 ± 0.1 (*0.9*)	nd nd	nd nd	nd nd	2.7 ± 0.1 (*2.5*)
850	fast	6 ± 1 (*2.0*)	6 ± 1 (*2.0*)	5 ± 1 (*1.8*)	6 ± 1 (*2.3*)	62 ± 3 (*44*)
	slow	0.8 ± 0.1 (*0.8*)	1.2 ± 0.3 (*1.2*)	1.2 ± 0.3 (*1.3*)	0.9 ± 0.1 (*1.1*)	2.9 ± 0.1 (*2.6*)

[a] nd, not determined.

the traces measured for the reaction of $HbFe^{II}NO$ with different amounts of O_2 (100−850 μM) were both essentially independent of the O_2 concentration (Table 1).

The rather large errors associated with the values of the rate constants discussed above, in particular with those of the fast component, were probably due to the difficulties encountered by fitting the single traces to a two-exponential expression. Indeed, reaction time courses that were apparently identical sometimes resulted in values of the fast component of the rate constants that varied by a factor of 2−3. Thus, we decided to calculate the two rate constants also from the negative slope of the plots of $\ln(A_t - A_\infty)$ versus time, for the beginning and for the end of the reaction, respectively. For all O_2 concentrations studied, with this method we obtained values of $\sim 2 \times 10^{-4}$ and $(0.8-1.2) \times 10^{-4}$ s^{-1} for the fast and the slow components of the observed rate constants, respectively. The value of the fast component was thus a factor of 2−3 lower than that obtained with the exponential fit, whereas the values of the slow components were nearly identical. These differences are clearly within the margin of error of the experiments. Taken together, these data confirm the lack of influence of the reaction rates on the O_2 concentration for the oxidation of $HbFe^{II}NO$.

The reaction between $HbFe^{II}NO$ and O_2 was also studied in the presence of different amounts of CO_2. The spectral changes were identical to those observed in the absence of added CO_2. Two isosbestic points around 523 and 602 nm were present only in the first 2−3 h of the reaction. For all O_2 and CO_2 concentrations studied, the final spectrum corresponded to that of pure metHb. As shown in Figures 3 and 4, the kinetic traces extracted at 544 nm for the reaction of 100 μM O_2 with 50 μM $HbFe^{II}NO$ did not depend on the concentration of CO_2 in the range 12−1200 μM and were identical to that obtained in the absence of added CO_2. In all cases, the apparent rate constants resulting from the two-exponential fits, summarized in Table 1, were nearly identical (within the errors of the measurements). Slightly larger values were found for the fast component of the reaction in the presence of 1.2 mM CO_2. A similar observation was done when 850 μM O_2 was used to oxidize $HbFe^{II}NO$. The rate constants obtained from the fits of the traces collected in

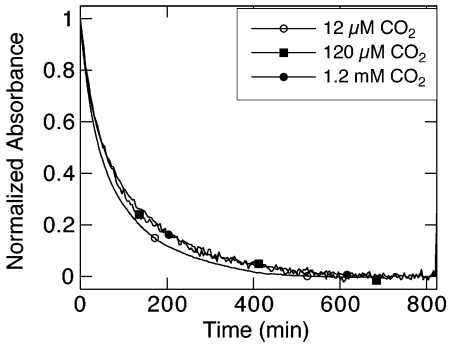

FIGURE 3: Normalized averaged time courses (at 544 nm) of the reactions of ~45 μM $HbFe^{II}NO$ with 100 μM O_2 in the presence of different CO_2 concentrations (given in the legend) in 0.1 M phosphate buffer, pH 7.2. Spectra were collected every 4 min.

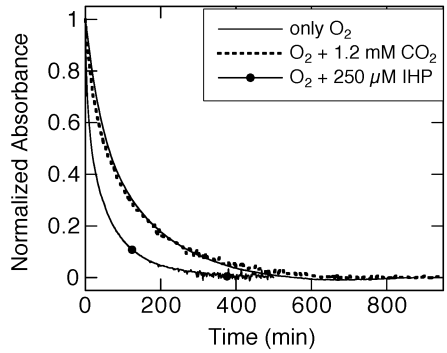

FIGURE 4: Normalized averaged time courses (at 544 nm) of the reactions of ~45 μM $HbFe^{II}NO$ with 100 μM O_2 in the absence and presence of 1.2 mM CO_2 or of 250 μM IHP in 0.1 M phosphate buffer, pH 7.2. Spectra were collected every 4 min.

the presence of CO_2 were nearly identical to those measured in its absence.

Also, for the experiments in the presence of different amounts of CO_2 the observed rate constants were determined additionally from the linear fit of the first and the last part of the plot of $\ln(A_t - A_\infty)$ versus time. As summarized in Table 1, in most cases the values of the fast and the slow components of the rate were 2×10^{-4} and $(1.1-1.3) \times 10^{-4}$ s^{-1}, respectively. In agreement with the results of the exponential fits, slightly larger values of the fast component were obtained in the presence of 1.2 mM CO_2 (2.4×10^{-4} and 2.3×10^{-4} s^{-1} for the reactions with 100 and 850 μM O_2, respectively). Nevertheless, these differences can be considered within the error of the experiments. In agreement with the observed lack of influence of CO_2, no changes were found in the reaction rates when the oxidation of $HbFe^{II}NO$ was started by adding an air-saturated solution or by simply transferring the solution in an air-filled vial.

Finally, we studied the influence of the strong allosteric effector IHP on the oxidation rate of $HbFe^{II}NO$. For this purpose, we first added 5 equiv of IHP (from a degassed aqueous solution) to the $HbFe^{II}NO$ solution. In agreement with previous reports (*19*), the two absorbance maxima of $HbFe^{II}NO$ shifted from 545 and 572 nm to 543 and 570 nm, respectively, and their absorbance decreased slightly. Upon addition of the O_2-containing solution we observed the gradual formation of metHb (Figure 5). As visible in the representative experiment depicted in Figure 5, the conversion of $HbFe^{II}NO$/IHP to metHb proceeded without clean isosbestic points. This feature may be due to the changes

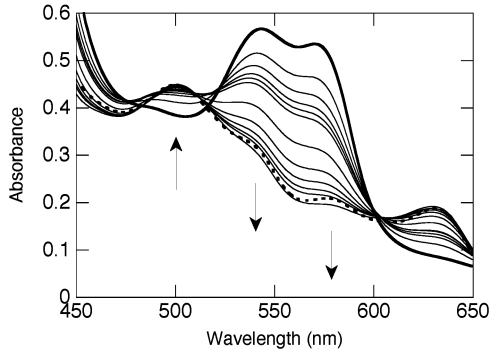

FIGURE 5: UV/vis spectra of the reaction of ~45 μM $HbFe^{II}NO$ with 100 μM O_2 in the presence of 250 μM IHP in 0.1 M phosphate buffer, pH 7.2. Conversion of $HbFe^{II}NO$ (bold line) to metHb (λ_{max} = 500 and 631 nm). The spectra depicted were collected immediately, 2 min, 4 min, 6 min, 8 min, 10 min, 30 min, 1 h, 1.5 h, 2 h, 2.5 h, and 4.5 h after mixing. Comparison with the spectrum of pure metHb (dotted bold line).

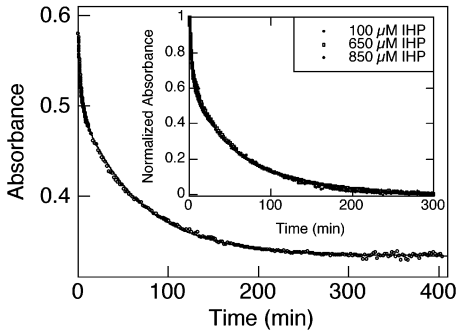

FIGURE 6: Time courses (at 544 nm) of the reactions of ~45 μM $HbFe^{II}NO$ with 850 μM O_2 in the presence of 250 μM IHP in 0.1 M phosphate buffer, pH 7.2. In one experiment, the data up to 11.5 min were collected every 7 s. In the second experiment, the whole reaction was studied by measuring a spectrum every 2 min. The fit of the combined data is shown as a line. Inset: Normalized averaged time courses (at 544 nm) of the reactions of ~45 μM $HbFe^{II}NO$ with 850, 650, or 100 μM O_2 in the presence of 250 μM IHP in 0.1 M phosphate buffer, pH 7.2.

observed in the absorbance spectrum of $HbFe^{II}NO$ upon addition of IHP (*18*, *20*).[2] Moreover, the last spectrum was very similar but not identical to that of pure metHb. Specifically, the absorbance maximum at 577 nm was slightly less pronounced (Figure 5). These absorbance changes were not due to the presence of IHP, since addition of 5 equiv of IHP to metHb did not induce any change in its absorption spectrum (data not shown).

As shown in Figure 4, addition of 5 equiv of IHP led to a significant increase in the oxidation rate of $HbFe^{II}NO$. To get more accurate values of the absorbance changes arising at the beginning of the reaction, the first 11.5 min were also studied separately by collecting a spectrum every 7 s in the range 542−547 nm. The kinetic traces extracted at 544 nm for the two experiments were then superimposed (Figure 6). These combined traces were also fitted well to a two-exponential expression. The value of the apparent rate constant for the fast component was approximately 1 order of magnitude larger than that obtained under identical conditions in the absence of IHP (Table 1). In contrast, the value of the slow component was only slightly larger in the presence of IHP (Table 1).

Interestingly, for the reactions in the presence of IHP, the oxidation rate of $HbFe^{II}NO$ by 100 μM O_2 was slightly lower than that measured with 650 and 850 μM O_2 (Table 1). To check whether this small difference was again due to the difficulties to get reliable values from the two-exponential fits, we also calculated the two observed rate constants from the linear fits of the plots of $\ln(A_t - A_\infty)$ versus time of the two sets of data (measured every 7 s for 11.5 min and every 4 min for 6−7 h), respectively. As summarized in Table 1, the observed rate constants calculated according to this procedure were essentially identical for all of the O_2 concentrations studied (for both the fast and the slow component). Moreover, as shown in the inset of Figure 6, the kinetic traces measured in the presence of 100, 650, or 850 μM O_2 were superimposable. Taken together, these data strongly indicate that in the presence of IHP the rates of the O_2-mediated oxidation of $HbFe^{II}NO$ are essentially independent of the O_2 concentration. Nevertheless, the data obtained up to now do not allow to exclude the possibility of a small O_2 concentration dependence in the presence of IHP.

Kinetic Studies of the Dissociation of NO• from $HbFe^{II}NO$ by CO Replacement. The kinetic studies reported above of the reaction of $HbFe^{II}NO$ with O_2 suggested that the rate-determining step of this oxidation does not involve a direct reaction with O_2 and may thus be represented by the dissociation of NO• from $HbFe^{II}NO$. To confirm this hypothesis we determined the dissociation rate of NO• from $HbFe^{II}NO$, under experimental conditions identical to those used above for the studies of the O_2-mediated oxidation of $HbFe^{II}NO$. Dissociation of NO• from $HbFe^{II}NO$ was studied spectrophotometrically by replacement with CO in the presence of an excess of dithionite. The absorbance changes were followed in the range 450−650 nm, and in most cases spectra were collected every 4 min. Upon addition of the CO/dithionite solution the spectrum of $HbFe^{II}NO$ gradually converted to that of $HbFe^{II}CO$, as confirmed by comparison with a $HbFe^{II}CO$ spectrum prepared by exposing deoxyHb to CO (data not shown). To determine the NO• dissociation rate constants, we extracted the reaction time courses at 480 nm. These kinetic traces were fitted reasonably well to a two-exponential expression. Nearly identical rates were observed by fitting the reaction time courses at 450 or 590 nm, two wavelengths at which no or minimal spectral changes are observed between fully and partially nitrosylated Hb (*18*). In the presence of 850 μM CO and 8.5 mM dithionite we obtained values of $(3.2 \pm 0.7) \times 10^{-4}$ and $(0.70 \pm 0.02) \times 10^{-4}$ s^{-1} for the two apparent rates, respectively. A slightly lower value for the fast component was obtained from the linear fit of the logarithmic plot (1.6×10^{-4} s^{-1}), whereas that of the slow component was nearly identical (0.8×10^{-4} s^{-1}). These values are very similar to those obtained for the O_2-mediated oxidation of $HbFe^{II}NO$ under identical

[2] Olson and co-workers have clearly shown that the spectrum of $HbFe^{II}NO$ is modified by addition of IHP (*20*). Indeed, in fully nitrosylated hemoglobin $Hb(Fe^{II}NO)_4$ IHP stabilizes the T-form of the protein and causes the complete rupture of the proximal His−Fe bonds in the α-subunits. Thus, because the UV/vis spectra of the 5- and the 6-coordinate nitrosyl complexes are slightly different, IHP induces changes in the spectrum of $HbFe^{II}NO$. Clearly, the extent of the spectral changes will depend on the amount of 5-coordinate α-$HbFe^{II}NO$ present in solution. During the oxidation reaction of $Hb(Fe^{II}NO)_4$, intermediates such as $Hb[(Fe^{III}OH_2)_2(Fe^{II}NO)_2]$ or $Hb[(Fe^{III}OH_2)_3(Fe^{II}NO)]$ will be formed. Since in its oxidized iron(III) form Hb favors the R-form, the amount of 5-coordinate α-$HbFe^{II}NO$ will vary during the course of the oxidation reaction, and thus, no clear isosbestic points can be observed.

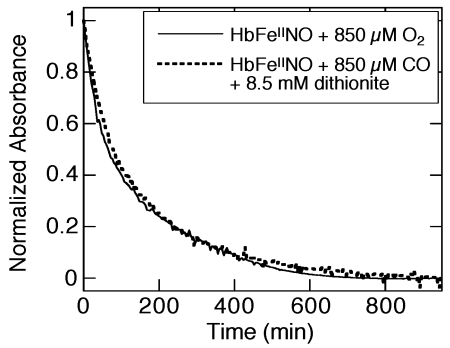

FIGURE 7: Normalized averaged time courses collected at 544 and 480 nm for the reactions of ~45 μM HbFe^{II}NO with O_2 and CO, respectively (in 0.1 M phosphate buffer, pH 7.2). Spectra were collected every 4 min.

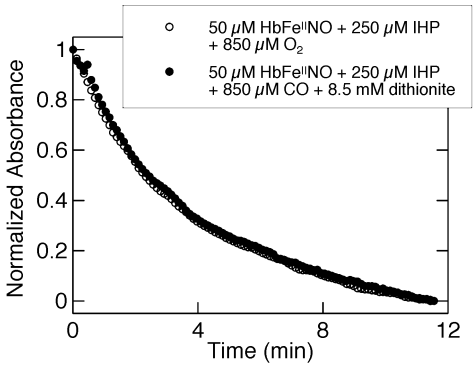

FIGURE 8: Normalized averaged time courses collected at 544 and 480 nm for the first 11.5 min of the reactions of ~45 μM HbFe^{II}NO with O_2 and CO in the presence of IHP (in 0.1 M phosphate buffer, pH 7.2). Spectra were collected every 7 s.

conditions (Table 1). Indeed, as shown in Figure 7, the normalized reaction time courses extracted at 544 and 480 nm for the O_2-mediated addition of HbFe^{II}NO and for the NO$^\bullet$ replacement by CO, respectively, were superimposable.

The dissociation rate of NO$^\bullet$ from HbFe^{II}NO has previously been shown to increase in the presence of the allosteric effector IHP (*21*). Under the conditions of our experiments (50 μM HbFe^{II}NO, 850 μM CO, and 8.5 mM dithionite) we also observed a significant increase of the fast component of the dissociation rate, $(25 \pm 1) \times 10^{-4}$ s^{-1}. In contrast, the value of the rate constant of the slow component was only slightly higher, $(0.98 \pm 0.01) \times 10^{-4}$ s^{-1}. These dissociation rates, measured in the presence of 5 equiv of IHP, were determined by fitting the combined averaged traces of the measurements of the first 11.5 min (collected every 7 s) and those of the whole reaction time (collected every 4 min). The linear fit of the logarithmic plot gave values in the same order of magnitude (44×10^{-4} and 0.94×10^{-4} s^{-1} for the fast and the slow component, respectively). Thus, also for the experiments in the presence of IHP, a good agreement exists between the rates of NO$^\bullet$ dissociation and those of the O_2-mediated oxidation of HbFe^{II}NO. As shown in Figure 8, essentially identical (normalized) reaction time courses were obtained in the first 11.5 min of these two reactions.

SNO-Hb Formation from the Reaction of HbFe^{II}NO with O_2. We have previously reported that, upon reaction with air, HbFe^{II}NO leads to nitrosation of Cysβ93 and thus formation of SNO-Hb (*14*). We have shown that O_2 is essential for SNO-Hb formation and have proposed that the reaction proceeds via dissociation of NO$^\bullet$ followed by reaction with O_2 to generate the nitrosating species $NO_2^\bullet$ and/or N_2O_3 (*14*). Thus, it is conceivable that SNO-Hb formation is more efficient if NO$^\bullet$ is bound to the β-subunit of Hb, since Cysβ93 is localized on the proximal side of the β-heme at ca. 10 Å from the iron center. It has been reported that equilibration of deoxyHb with substoichiometric amounts of NO$^\bullet$ first leads to the formation of both 5- and 6-coordinate nitrosyl complexes (of the α- and the β-subunit, respectively) (*20*, *22*, *23*), consistent with a lack of cooperativity for NO$^\bullet$ binding to deoxyHb (*24*). However, about 40% of the NO$^\bullet$ molecules initially bound to the β-subunits subsequently transfer to the α-subunits, and the final product of the reaction between deoxyHb and substoichiometric amounts of NO$^\bullet$ corresponds quantitatively to the 5-coordinate α-subunit nitrosyl complex (*20*, *22*, *23*). The half-time of this rearrangement is on the order of 7−10 min (*20*). In a recent study, 60 min was needed to get complete transfer of NO$^\bullet$ to the hemes of the α-subunit, but the longer time was mainly due to a different experimental setup, which first required diffusion of NO$^\bullet$ into the deoxyHb solution, probably the rate-determining step in this system (*23*).

To investigate whether migration of NO$^\bullet$ from the β- to the α-subunit influenced the SNO-Hb yields after exposing partially nitrosylated Hb to air, we added 0.1 equiv of NO$^\bullet$ (from a saturated NO$^\bullet$ solution) to a deoxyHb solution and incubated the reaction mixture either for 0, for 10, or for 60 min.[3] Surprisingly, analysis of the *S*-nitrosothiol content immediately after exposure of the samples to air showed that the SNO-Hb yields did not depend on the time waited after addition of NO$^\bullet$ to deoxyHb (0, 10, or 60 min). For all three samples we obtained approximately 9% of Cysβ93−NO, relative to the NO$^\bullet$ concentration added. Thus, apparently the extent of nitrosation of Cysβ93 does not depend on whether NO$^\bullet$ is bound to the α- or to the β-subunit.

In a further set of experiments, in analogy to the kinetic experiments reported above, we studied the influence of the amounts of O_2 and of CO_2 on the SNO-Hb yields obtained upon exposure of HbFe^{II}NO to air/O_2. For this purpose, we treated (under anaerobic conditions) a HbFe^{II}NO solution with the amount of an O_2-saturated aqueous solution required to get a final O_2 concentration of ~220 μM, which corresponds to the O_2 concentration of an air-equilibrated solution. The Cysβ93−NO yields were nearly identical to those obtained under similar conditions by exposing the HbFe^{II}NO solution to air. For the samples analyzed immediately after exposure of the oxidant we obtained relative Cysβ93−NO yields of 1.3 ± 0.1% and 1.5 ± 0.1% (relative to the amount of NO$^\bullet$ added) for the experiments with O_2 and air, respectively. When we waited 10 min before analyzing the samples, in agreement with previous reports (*14*), the Cysβ93−NO yields were both slightly higher. We obtained 1.9 ± 0.2% and 2.2 ± 0.5% (relative to the amount of NO$^\bullet$ added) for the experiments with O_2 and air, respectively. Addition of larger amounts of O_2 (850 μM) led again to nearly identical yields (2.1 ± 0.1%, relative to the amount of NO$^\bullet$ added).

[3] In our previous work (*14*), we have shown that for the reactions of NO$^\bullet$ with deoxyHb the SNO-Hb yields do not depend on the procedure used to add the NO$^\bullet$ solution.

Table 2: SNO-Hb Yields[a] Obtained from Reaction of $HbFe^{II}NO$ (50 μM) with Different Amounts of O_2 in the Absence or Presence of Different Amounts of CO_2

$[O_2]$ (μM)	$[CO_2]$ (μM)	SNO-Hb yields (%)
220	12	3.0 ± 0.1
220	120	3.0 ± 0.1
850	12	3.2 ± 0.1
850	120	3.2 ± 0.1

[a] % relative to the amount of $NO^{\bullet}$ added.

Scheme 1

$$HbFe^{II}NO + O_2 \rightleftharpoons HbFe^{II} + NO^{\bullet} + O_2 \rightleftharpoons HbFe^{II}O_2 + NO^{\bullet} \longrightarrow HbFe^{III} + NO_3^-$$

Scheme 2

$$MbFe^{II}NO + O_2 \longrightarrow \{MbFe^{III}N(O)OO^-\} \longrightarrow MbFe^{III} + NO_3^-$$

The influence of CO_2 was studied for both the reactions with 220 and with 850 μM O_2. As summarized in Table 2, addition of 12 or 120 μM CO_2 did not influence the SNO-Hb yields. The influence of IHP on the SNO-Hb yields could not be studied, as for unclear reasons IHP was found to interfere with the Saville analysis of *S*-nitrosothiols.

DISCUSSION

Hemoglobin has long been thought to represent a sink for $NO^{\bullet}$, by rapidly converting it to nitrate through its irreversible reaction with oxyHb (*3*−*5*). However, under physiological as well as pathophysiological conditions $NO^{\bullet}$ can also be trapped by deoxyHb and thus generate its nitrosylated form $HbFe^{II}NO$. This hemoglobin derivative is rather stable, and it dissociates $NO^{\bullet}$ at a very slow rate. We have recently shown that faster release of $NO^{\bullet}$ can occur upon oxidation of $HbFe^{II}NO$ by peroxynitrite (*25*). This reaction leads to oxidation of the iron center to produce $HbFe^{III}NO$, from which $NO^{\bullet}$ dissociates at a rate 4 orders of magnitude larger than that for dissociation from $HbFe^{II}NO$ (*25*).

The kinetic studies presented in this work strongly suggest that dissociation of $NO^{\bullet}$ is the rate-determining step also of the O_2-mediated oxidation of $HbFe^{II}NO$. Indeed, the rate of this oxidation does not depend on the O_2 concentration. Thus, our data are consistent with the mechanism displayed in Scheme 1, that is, dissociation of $NO^{\bullet}$ (rate-determining step), rapid binding of O_2 to deoxyHb, and subsequent $NO^{\bullet}$-mediated oxidation of oxyHb to metHb and NO_3^-.

Interestingly, the analogous reaction of $MbFe^{II}NO$ with O_2 has been suggested to proceed according to Scheme 2 via an intermediate, assigned as the N-bound peroxynitrite−iron(III) complex $[MbFe^{III}N(O)OO^-]$ (*12*). The UV/vis spectrum of this intermediate, calculated by singular value decomposition, is very similar to that observed spectrophotometrically in the course of the reaction of oxyMb with $NO^{\bullet}$ and assigned as the O-bound peroxynitrite−metMb complex $MbFe^{III}OONO$ (*2*). The rate constants for the formation of $[MbFe^{III}N(O)OO^-]$ [from the oxidation of MbFe(II)NO in an atmosphere saturated with pure O_2] and for its isomerization to metMb and nitrate are 1.34×10^{-3} and 2.82×10^{-3} s^{-1}, at pH 7.0 and 37 °C (*12*). However, the similarity of the rate of formation of $[MbFe^{III}N(O)OO^-]$ to that of $NO^{\bullet}$ dissociation from $MbFe^{II}NO$ [1.2×10^{-4} s^{-1}, at pH 7.0 and 22 °C (*18*)] has led to the suggestion that also this reaction

Scheme 3

$$MbFe^{II}NO + O_2 \rightleftharpoons \{MbFe^{II}O_2/NO^{\bullet}\} \longrightarrow MbFe^{III} + NO_3^-$$

may proceed according to the pathway proposed here for the reaction of O_2 with $HbFe^{II}NO$ (Scheme 1) (*26*).

Møller and Skibsted recently reinvestigated the O_2-mediated oxidation of $MbFe^{II}NO$ and proposed an alternative mechanism (*13*). Indeed, these authors found that the rate of the first reaction step is linearly dependent on the O_2 concentration at low concentrations, whereas for O_2 concentrations higher than 220 μM (atmospheric oxygen pressure) the rate displayed a saturation behavior (*13*). Moreover, the rate of the second reaction step was found to be independent of the O_2 concentration. These data are in agreement with the mechanism given in Scheme 3, in which $NO^{\bullet}$ is first displaced by O_2 but stays trapped in a protein cavity close to the heme and, in the second step, reacts with oxyMb to metMb and nitrate (*13*). This mechanism is rather similar to that proposed in this work for the analogous reaction with $HbFe^{II}NO$ (Scheme 1).

The dissociation of $NO^{\bullet}$ from $HbFe^{II}NO$ has previously been studied by Moore and Gibson (*18*). These authors established that the $NO^{\bullet}$ dissociation rate from $HbFe^{II}NO$ can be measured in the presence of an excess of both dithionite and CO, the method we used in this work. The dissociation rates were essentially independent of the dithionite concentration (up to 115 mM) only in the presence of excess CO, which traps $HbFe^{II}$ and thus precludes competition between dithionite and $HbFe^{II}NO$ for free $NO^{\bullet}$ (*18*). Moore and Gibson determined the dissociation rate of $NO^{\bullet}$ from isolated subunits of Hb and found a difference between the values for the α- and the β-subunit (4.6×10^{-5} and 2.2×10^{-5} s^{-1}, respectively, at pH 7.0 and 22 °C) (*18*). In the same study, it was reported that the replacement of $NO^{\bullet}$ by CO in tetrameric $HbFe^{II}NO$ is biphasic at neutral pH. The rate of the slow phase, attributed to the dissociation from R-state molecules, was measured as 10^{-5} s^{-1}. Sharma and Ranney also studied the dissociation of $NO^{\bullet}$ from $HbFe^{II}NO$, by replacing $NO^{\bullet}$ with CO in the presence of dithionite (*21*). The initial fast phase observed in the reaction time courses was attributed to the presence of a small amount of T-state $HbFe^{II}NO$, in agreement with Moore and Gibson (*18*). The observation that even in the absence of IHP a small fraction of the nitrosyl complex of the α-chain is 5-coordinated supports this hypothesis. Indeed, the bond between the proximal His and the iron center can be ruptured only in the T-state. The observed rate constant for the slow phase, 1.8×10^{-5} s^{-1}, was attributed to the dissociation of $NO^{\bullet}$ from $Hb[(Fe^{II}CO)_3(Fe^{II}NO)]$. The values that we obtained in the present study for the two components of the $NO^{\bullet}$ dissociation rate as well as of the O_2-mediated oxidation of $HbFe^{II}NO$ were nearly 1 order of magnitude larger than those reported previously. No explanation was found for this discrepancy. However, the major difference between these data is that in our experiments we collected a significantly larger number of spectra, particularly at the beginning of the reaction.

The $NO^{\bullet}$ dissociation from $HbFe^{II}NO$ in the presence of IHP has previously been shown to be also a biphasic process (*21*). By using the $NO^{\bullet}$ replacement reaction with CO (in the presence of excess dithionite), the observed rates of the fast and the slow process were determined as 35×10^{-4} and 3.5×10^{-5} s^{-1}, respectively (*21*). In contrast, in the same

work the two observed rates were found to be $(30 \pm 10) \times 10^{-4}$ and $(1.0 \pm 0.3) \times 10^{-4}$ s^{-1}, respectively, with deoxyMb as the NO• scavenger (*21*). No comments were made on the discrepancy between the values of the slow reaction rates measured with the two different methods. The values determined in this work for the two components of the NO• dissociation rate in the presence of IHP were in good agreement with those measured with the deoxyMb method (*21*).

Binding of IHP to $HbFe^{II}NO$ induces the R to T transition and influences ligand affinity mainly of the α-chains and, to a lesser extent, of the β-chains. Indeed, in the T-form of $HbFe^{II}NO$ the tension on the heme is much larger in α- than in β-chains and, thus, leads to the cleavage of the His−Fe bond in the α-subunits. Consequently, the fast phase was attributed to the dissociation of NO• from α-chains, and the slow phase, which is less affected by addition of IHP, was ascribed with dissociation from β-chains. A similar effect of IHP has been reported for the rates of dissociation of O_2 from $HbFeO_2$. Despite the fact that O_2 dissociation is faster from β-chains than from α-chains, addition of IHP affects the dissociation rate from α-chains to a larger extent (*27*).

The consistency between the rates for O_2-mediated oxidation of $HbFe^{II}NO$ and those for NO• dissociation also in the presence of IHP further supports our mechanistic hypothesis based in Scheme 1. The difference between the values of the rates of the slow component of the two reactions may derive from a different kind of interaction of IHP with intermediate products of the two reactions, that is, $Hb[(Fe^{II}NO)_2(Fe^{III}OH_2)_2]$ and $Hb[(Fe^{II}NO)_2(Fe^{II}CO)_2]$, for the oxidation of $HbFe^{II}NO$ and NO• dissociation, respectively.

The in vivo concentration of $HbFe^{II}NO$ in humans and the physiological function of this Hb form are matters of debate. One study reported that the $HbFe^{II}NO$ concentration is approximately 5 μM in mixed venous blood and 2.5 μM in arterial blood (*28*). In another recent paper, $HbFe^{II}NO$ levels were found to be below the limit of detection by EPR spectroscopy (<1 μM) (*29*). Conflicting reports have been published also on the presence of a concentration gradient in venous vs arterial blood (*28*−*30*). Such a gradient is essential to support the theory according to which NO• binds to the heme when Hb is in the R-form (arterial blood) and is then transferred intramolecularly to Cysβ93 (to form SNO-Hb) when Hb is in the T-state in venous blood (*28*).

Under pathological conditions, a venous vs arterial gradient was found in congestive heart failure patients (*31*) and in a rat model of endotoxemic sepsis (*32*). Thus, in vivo $HbFe^{II}NO$ may undergo a fast reaction that causes the buildup of the observed gradient. The largest rate constants determined in this work for NO• dissociation or for oxidation of $HbFe^{II}NO$, in the presence of the allosteric effector IHP, indicate that the half-life of these reactions is ca. 3 min. Thus, these reactions are clearly too slow to explain the observed gradient. It has recently been argued (*32*) that in vivo either NO• dissociation occurs at a faster rate than in vitro or there is a fast reaction between $HbFe^{II}NO$ and oxygen. Alternatively, $HbFe^{II}NO$ may be oxidized to $HbFe^{III}NO$, from which NO• would dissociate with a half-life of ca. 1 s (*25*).

The observation that Cysβ93 is S-nitrosated upon reaction of $HbFe^{II}NO$ with NO• further supports the mechanism based on NO• dissociation as the first reaction step. Interestingly, previous experiments showed that the Cysβ93−NO yields did not change significantly when $HbFe^{II}NO$ was allowed to react with air for either 10 or 60 min (*14*). Longer reaction times (several hours) even led to a decrease of the SNO-Hb yields. Taken together, our data suggest that the lack of correlation between the extent of $HbFe^{II}NO$ oxidation and the SNO-Hb yields is likely to be due to the instability of SNO-Hb under our experimental conditions (*33*).

The experiments reported here with substoichiometric amounts of NO• and different reaction times after addition of NO• to deoxyHb suggest that under these conditions the SNO-Hb yields do not depend on whether NO• is coordinated to the α- or to the β-heme. Moreover, these results are surprising since they show that SNO-Hb can be generated even in the presence of oxyHb. Indeed, upon exposure of the mixture of deoxyHb and 0.1 equiv NO• to O_2, large quantities of oxygenated heme centers are produced. Even under these conditions, our data indicate that NO• dissociates from $HbFe^{II}NO$ and does not react exclusively with $HbFeO_2$ to produce nitrate but also generates 9% SNO-Hb (relative to the amount of NO• added). Surprisingly, this pathway seems to be followed even when NO• is bound to the α-subunits.

It has previously been shown that NO• can be trapped in hydrophobic pockets of Mb (*34*). Thus, an alternative explanation for the formation of SNO-Hb in these experiments with substoichiometric amounts of NO• is that NO• is partly trapped in a hydrophobic pocket close to Cysβ93 and leads to nitrosation of this residue upon reaction with O_2. Since no differences were found between the SNO-Hb yields obtained by allowing NO• to interact with deoxyHb only a few seconds or 60 min, this noncovalent interaction should be rather strong.

In conclusion, we have shown that the rate of oxidation of $HbFe^{II}NO$ by O_2 does not depend on the O_2 concentration in the range 100−850 μM. The values of the rate constants obtained for the α- and the β-chains were approximately 2×10^{-4} and 1×10^{-4} s^{-1}, respectively. Because of the different kind of interaction of IHP with the two subunits of Hb, in the presence of IHP, the value for the α-chain was significantly larger (44×10^{-4} s^{-1}) whereas that for the β-chain was only slightly higher (2.5×10^{-4} s^{-1}). Both in the absence and in the presence of IHP, the rates of the O_2-mediated oxidation of $HbFe^{II}NO$ were essentially identical to those of NO• dissociation from $HbFe^{II}NO$, determined under analogous conditions by replacement of NO• with CO in the presence of an excess of dithionite. Taken together, our data show that the reaction between O_2 and $HbFe^{II}NO$ proceeds in three steps via dissociation of NO• (rate-determining step), binding of O_2 to deoxyHb, and NO•-mediated oxidation of oxyHb to metHb and nitrate.

ACKNOWLEDGMENT

We thank APEX Bioscience, Inc., for the supply of purified human hemoglobin.

REFERENCES

1. Moncada, S., Palmer, R. M. J., and Higgs, E. A. (1991) Nitric oxide: physiology, patophysiology, and pharmacology, *Pharmacol. Rev. 43*, 109−142.
2. Herold, S., Exner, M., and Nauser, T. (2001) Kinetic and mechanistic studies of the NO•-mediated oxidation of oxymyoglobin and oxyhemoglobin, *Biochemistry 40*, 3385−3395.

3. Lancaster, J. R., Jr. (1994) Simulation of the diffusion and reaction of endogenously produced nitric oxide, *Proc. Natl. Acad. Sci. U.S.A. 91*, 8137−8141.
4. Beckman, J. S. (1996) in *Nitric Oxide: Principles and Actions* (Lancaster, J., Jr., Ed.) pp 1−82, Academic Press, San Diego.
5. Liu, X., Miller, M. J. S., Joshi, M. S., Sadowska-Krowicka, H., Clark, D. A., and Lancaster, J. R., Jr. (1998) Diffusion-limited reaction of free nitric oxide with erythrocytes, *J. Biol. Chem. 273*, 18709−18713.
6. Gow, A. J., and Stamler, J. S. (1998) Reactions between nitric oxide and hemoglobin under physiological conditions, *Nature 391*, 169−173.
7. Gow, A. J., Luchsinger, B. P., Pawloski, J. R., Singel, D. J., and Stamler, J. S. (1999) The oxyhemoglobin reaction of nitric oxide, *Proc. Natl. Acad. Sci. U.S.A. 96*, 9027−9032.
8. Nagababu, E., Ramasamy, S., Abernethy, D. R., and Rifkind, J. M. (2003) Active nitric oxide produced in the red cell under hypoxic conditions by deoxyhemoglobin-mediated nitrite reduction, *J. Biol. Chem. 278*, 46349−46356.
9. Cosby, K., Partovi, K. S., Crawford, J. H., Patel, R. P., Reiter, C. D., Martyr, S., Yang, B. K., Waclawiw, M. A., Zalos, G., Xu, X., Huang, K. T., Shields, H., Kim-Shapiro, D. B., Schechter, A. N., Cannon, R. O., III, and Gladwin, M. T. (2003) Nitrite reduction to nitric oxide by deoxyhemoglobin vasodilates the human circulation, *Nat. Med. 9*, 1497−1505.
10. Killday, K. B., Tempesta, M. K., Bailey, M. E., and Metral, C. J. (1988) Structural characterization of nitrosylhemochromogen of cooked cured meat: Implications in the meat-curing reaction, *J. Agric. Food Chem. 36*, 909−914.
11. Kanner, J., Harel, S., Shagolovich, J., and Berman, S. (1984) Antioxidative effects of nitrite in cured meat products: nitric oxide-iron complexes of low molecular weight, *J. Agric. Food Chem. 32*, 512−515.
12. Arnold, E. V., and Bohle, D. S. (1996) Isolation and oxygenation reactions of nitrosylmyoglobins, *Methods Enzymol. 269*, 41−55.
13. Møller, J. K. S., and Skibsted, L. H. (2004) Mechanism of nitrosylmyoglobin autoxidation: temperature and oxygen pressure effects on the two consecutive reactions, *Chem. Eur. J. 10*, 2291−2300.
14. Herold, S., and Röck, G. (2003) Reactions of deoxy-, oxy-, and methemoglobin with nitrogen monoxide. Mechanistic studies of the S-nitrosothiol formation under different mixing conditions, *J. Biol. Chem. 278*, 6623−6634.
15. Antonini, E., and Brunori, M. (1971) *Hemoglobin and Myoglobin in Their Reactions with Ligands*, North-Holland, Amsterdam.
16. Saville, B. (1958) A scheme for the colorimetric determination of microgram amounts of thiols, *Analyst (London) 83*, 670−672.
17. Harned, H. S., and Bonner, F. T. (1945) The first ionization of carbonic acid in aqueous solutions of sodium chloride, *J. Am. Chem. Soc. 67*, 1026−1031.
18. Moore, E. G., and Gibson, Q. H. (1976) Cooperativity in the dissociation of nitric oxide from hemoglobin, *J. Biol. Chem. 251*, 2788−2794.
19. Perutz, M. F., Kilmartin, J. V., Nagai, K., Szabo, A., and Simon, S. R. (1976) Influence of globin structures on the state of the heme ferrous low spin derivatives, *Biochemistry 15*, 178−187.
20. Hille, R., Olson, J. S., and Palmer, G. (1979) Spectral transitions of nitrosyl hemes during ligand binding to hemoglobin, *J. Biol. Chem. 254*, 12110−12120.
21. Sharma, V. S., and Ranney, H. M. (1978) The dissociation of NO from nitrosylhemoglobin, *J. Biol. Chem. 253*, 6467−6472.
22. Taketa, F., Antholine, W. E., and Chen, J. Y. (1978) Chain nonequivalence in binding of nitric oxide to hemoglobin, *J. Biol. Chem. 253*, 5448−5451.
23. Fago, A., Crumbliss, A. L., Peterson, J., Pearce, L. L., and Bonaventura, C. (2003) The case of the missing NO-hemoglobin: Spectral changes suggestive of heme redox reactions reflect changes in NO-heme geometry, *Proc. Natl. Acad. Sci. U.S.A. 100*, 12087−12092.
24. Hille, R., Palmer, G., and Olson, J. S. (1977) Chain equivalence in reaction of nitric oxide with hemoglobin, *J. Biol. Chem. 252*, 403−405.
25. Herold, S. (2004) The outer-sphere oxidation of nitrosyliron(II) hemoglobin by peroxynitrite leads to the release of nitrogen monoxide, *Inorg. Chem. 43*, 3783−3785.
26. Ford, P. C., and Lorkovic, I. M. (2002) Mechanistic aspects of the reactions of nitric oxide with transition-metal complexes, *Chem. Rev. 102*, 993−1018.
27. Olson, J. S., Andersen, M. E., and Gibson, Q. H. (1971) The dissociation of the first oxygen molecule from some mammalian oxyhemoglobins, *J. Biol. Chem. 246*, 5919−5923.
28. McMahon, T. J., Moon, R. E., Luschinger, B. P., Carraway, M. S., Stone, A. E., Stolp, B. W., Gow, A. J., Pawloski, J. R., Watke, P., Singel, D. J., Piantadosi, C. A., and Stamler, J. S. (2002) Nitric oxide in the human respiratory cycle, *Nat. Med. 8*, 711−717.
29. Xu, X., Cho, M., Spencer, N. Y., Patel, N., Huang, Z., Shields, H., King, S. B., Gladwin, M. T., Hogg, N., and Kim-Shapiro, D. B. (2003) Measurements of nitric oxide on the heme iron and {beta}-93 thiol of human hemoglobin during cycles of oxygenation and deoxygenation, *Proc. Natl. Acad. Sci. U.S.A. 100*, 11303−11308.
30. Jaszewski, A. R., Fann, Y. C., Chen, Y.-R., Sato, K., Corbett, J., and Mason, R. P. (2003) EPR spectroscopy studies on the structural transition of nitrosyl hemoglobin in the arterial-venous cycle of DEANO-treated rats as it relates to the proposed nitrosyl hemoglobin/nitrosothiol hemoglobin exchange, *Free Radical Biol. Med. 35*, 444−451.
31. Datta, B., Tufnell-Barrett, T., Bleasdale, R. A., Jones, C. J. H., Beeton, I., Paul, V., Frenneaux, M., and James, P. (2004) Red blood cell nitric oxide as an endocrine vasoregulator. A potential role in congestive heart failure, *Circulation 109*, 1339−1342.
32. Davies, N. A., Brealey, D. A., Stidwill, R., Singer, M., Svistunenko, D. A., and Cooper, C. E. (2005) Nitrosyl heme production compared in endotoxemic and hemorragic shock, *Free Radical Biol. Med. 38*, 41−49.
33. Gladwin, M. T., Wang, X., Reiter, C. D., Yang, B. K., Vivas, E. X., Bonaventura, C., and Schechter, A. N. (2002) S-Nitrosohemoglobin is unstable in the reductive erythrocyte environment and lacks O_2/NO-linked allosteric function, *J. Biol. Chem. 277*, 27818−27828.
34. Sampath, V., Zhao, X.-J., and Caughey, W. S. (2001) Anesthetic-like interactions of nitric oxide with albumin and hemeproteins. A mechanism for control of protein function?, *J. Biol. Chem. 276*, 13635−13643.

BI0475929